

# Diffusive torsional dynamics of malachite green molecules in solid matrices probed by fluorescence decay

Kazi Monowar Abedin,<sup>a)</sup> Jing Yong Ye,<sup>a)</sup> Hideyuki Inouye,<sup>a)</sup> Toshiaki Hattori,<sup>a)</sup> Hitoshi Sumi,<sup>b)</sup> and Hiroki Nakatsuka<sup>a),c)</sup>

University of Tsukuba, Tsukuba 305, Japan

(Received 27 December 1994; accepted 14 July 1995)

The torsional dynamics of phenyl rings of malachite green molecules in the excited state is studied in polymeric and monomeric glass matrices by measuring the fluorescence decay time as a function of temperature. It is shown that the phenyl rings rotate diffusively in solid polymers (polymethyl methacrylate and polyvinyl alcohol) quite rapidly even at low temperatures. To analyze the experimental results, we used the concept of microviscosity which controls the diffusive rotational motion of phenyl rings of malachite green molecules in solid matrices. By using the reaction-rate theory, we show that a horizontal excited-state potential surface rather than a downhill potential surface for the rotation of phenyl rings can more reasonably explain the rotational motion in polymers. If we assume that the potential is horizontal, the temperature dependence of the microviscosity can be described by Andrade equation with a definite activation energy which is known to be valid for many liquids over a wide range of temperatures. This implies that the microscopic dynamics of small molecular rotations in a solid polymer resembles the behavior in many liquids. By monitoring the fluorescence decay of malachite green molecules doped in ethanol monomeric glass during its phase transition, we show that the effects of phase transition are well represented in the fluorescence decay time. We then propose to use malachite green molecules as sensitive optical microprobes of local dynamics in various solid matrices and their phase transitions, etc. © 1995 American Institute of Physics.

## I. INTRODUCTION

Dynamics of chromophores doped in amorphous materials is a topic of considerable current interest. Moreover, doped polymer films are expected to be utilized in future optical functional devices, for example, in persistent spectral hole burning (PSHB) memories. In these applications, it is very important to know how rigidly the doped chromophores (guest) are bound to the surrounding matrix. The nature of the guest–matrix interaction, on which this rigidity depends, is not so well understood in amorphous systems. In doped systems, the motion of the doped molecules or their constituents is influenced by the surrounding matrix. Molecular motions having no internal potential barrier are ideal probes of matrix rigidity, since matrix friction is the only impediment to molecular motions in these cases.

Malachite green (MG) is one of the dyes of the triphenylmethane (TPM) group where the central carbon atom is joined by three phenyl rings. When dissolved in ordinary liquids with low viscosities like water, ethanol, etc., and optically excited to the  $S_1$  electronic state, these dye molecules were observed to return to the ground  $S_0$  state without emitting almost any light.<sup>1,2</sup> This rapid radiationless process is caused by internal conversion and was shown to occur due to viscosity-dependent rotation of the phenyl rings around their axes<sup>3</sup> (Fig. 1). The required amount of rotation for the internal conversion process to occur was estimated to be roughly 10 degrees.<sup>4</sup> In liquids of low viscosities, the rotation occurs

very fast and the excited-state lifetime is very short (a few picoseconds). As the viscosity of the surrounding medium increases, the rotations of the phenyl rings are progressively retarded and the excited-state lifetime approaches the radiative lifetime of the dye.

Many researchers<sup>4–20</sup> have studied the excited-state dynamics of triphenylmethane dyes in various liquid systems, either by pump–probe methods or fluorescence decay methods. Some of the researchers found linear dependence of nonradiative decay time on the viscosity,<sup>4,10,13</sup> but a sublinear dependence at higher viscosities for higher alcohols was also observed.<sup>4,13</sup> This behavior was attributed to the difference between microviscosity and macroviscosity, i.e., the viscosity experienced by the rotating phenyl rings (microviscosity) was supposed to be different from macroscopic viscosity for these alcohols. Initially Sundstrom *et al.*<sup>13</sup> surmised from their experimental results that some barrier existed for the internal conversion in the excited-state potential surface of malachite green when dissolved in long-chained alcohols, but later Ben-Amotz and Harris<sup>4</sup> showed that the experimental data can be consistently explained without invoking the formation of barrier if one assumes that microviscosity experienced by phenyl rings in long-chained alcohols is different from their bulk macroviscosity. It now appears that the generally accepted opinion regards the excited-state potential of TPM dyes as being barrierless.

There have been a few theoretical treatments to describe the dynamics on a barrierless potential. For example, Bagchi, Fleming, Oxtoby (BFO)<sup>21</sup> argued about the decay kinetics on the assumptions that the excited-state potential surface is parabolic and the motion of the excited-state population after optical excitation on this surface is all-downhill toward a

<sup>a)</sup>Institute of Applied Physics.

<sup>b)</sup>Institute of Materials Science.

<sup>c)</sup>Author to whom correspondence should be addressed.

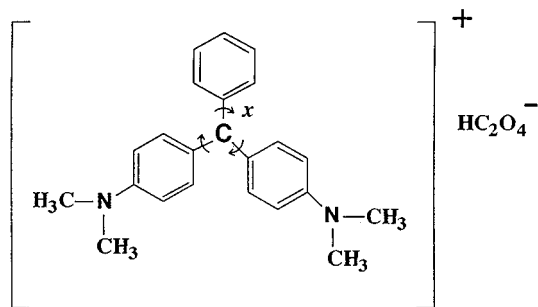


FIG. 1. Molecular structure of malachite green (oxalate). The curved arrows indicate rotational motion of the phenyl rings which brings about the internal conversion process.

sink. On the other hand, Ben-Amotz and Harris<sup>17</sup> assumed a horizontal excited-state potential surface and considered only the diffusive spreading of the excited-state population on this surface before its annihilation at a sink.

Concerning the use of TPM dye molecules as a probe of local microscopic environment, Huston, Justus, and Campillo<sup>22</sup> employed crystal violet molecules as a “molecular sensor” of the surrounding environment in glycerol solution when a shock wave excited by a laser pulse impinged on it. They evaluated the change in effective viscosity induced by the shock wave by measuring the fluorescence lifetime of crystal violet.

In contrast to liquids, there have been only a few studies of time-resolved excited-state dynamics of TPM dyes in solid matrices. One of the few examples we are aware of is due to Canva *et al.*,<sup>23,24</sup> who probed the excited-state population of malachite green in a sol-gel glass matrix by pump-probe methods at room temperature and derived a tentative value of local, or microviscosity of the matrix to the phenyl ring rotation of malachite green. Another example is due to Kemnitz and Yoshihara,<sup>25</sup> who studied the fluorescence decay dynamics of malachite green molecules adsorbed on quartz surfaces. The decay was found to be bi- or triexponential, and the authors argued that this behavior arises from microscopic site dependence of the adsorbed molecules on the surface.

There have been many reports on depolarization of chromophores (dye molecules) doped in polymer melts or solutions.<sup>26–29</sup> One of these is the paper by Barkowski, Mersch, and Dorfmueller,<sup>28</sup> who measured the fluorescence depolarization of 9-cyananthracene molecules in cyclohexane solution of polybutadiene as a function of temperature. They showed that the rotational relaxation time cannot be described by the Stokes-Einstein-Debye equation with the macroscopic viscosity in polymer solutions. Their implication is that macroviscosity of the polymer solution measured by mechanical experiments is different from the microviscosity experienced by the chromophores in the polymer solution. It may be appropriate to use the latter in the Stokes-Einstein-Debye equation. Several other researchers<sup>26,27,29</sup> have also pointed out the difference between bulk viscosity (measured by mechanical experiments) and local, or microviscosity experienced by chromophore molecules in long-chained polymers.

In this study, we performed fluorescence decay measurements of malachite green doped in solid matrices. We show that phenyl rings of malachite green can rotate in polymers quite rapidly even at low temperatures but cannot rotate rapidly in a monomer glass once it is completely frozen. We use the concept of microviscosity of the host which controls the rotational diffusion of the phenyl rings on the  $S_1$  potential surface in solid matrices. By comparing our experimental results with the results of the reaction-rate theory, we suggest that the rotational motion of the phenyl rings on the  $S_1$  potential surface in the solid matrices can be described by a diffusive motion on a horizontal potential surface. By monitoring the fluorescence decay of malachite green doped in ethanol monomeric glass during its phase transition process, we will show that the effects of the phase transition is well represented in the fluorescence decay time. We then propose to use MG molecules as molecular probes to examine the local dynamics of various solid matrices and their phase transitions, etc.

## II. EXPERIMENT AND RESULTS

In the present study, we doped malachite green molecules into three different solid matrices: polymethyl methacrylate (PMMA), polyvinyl alcohol (PVA), and ethanol glass (EtOH) and performed time resolved fluorescence experiments.

MG/PMMA samples were prepared by mixing 1 ml of concentrated (1 gm/l) MG solution in methanol with about 50 ml of PMMA solution (100 gm/l) in methylene chloride (CH<sub>2</sub>Cl<sub>2</sub>). The degree of polymerization of PMMA was about 7000. After mixing, the solution was poured into a small chalet and left to dry slowly. After overnight drying, a thin film sample was obtained. Films were 0.1–0.2 mm in thickness and transmission at 633 nm (He-Ne laser) was about 30%. MG/PVA samples were prepared in the same way except that the solvent for PVA (degree of polymerization 500) was water and the drying period was several days. A small amount of hydrochloric acid was added during the mixing process in this case to lower the pH to about 4 in order to prevent the formation of transparent carbinol form of MG.<sup>30</sup> Film thicknesses were about 0.2 mm and transmission at 633 nm wavelength was about 30%.

The schematic diagram of the fluorescence decay experiment is shown in Fig. 2. A YAG laser (Coherent, Antares) generated cw mode-locked pulses at a wavelength of 1064 nm. After frequency doubling, the second harmonic light was used to excite a synchronously pumped, hybrid mode-locked dye laser (Coherent, Satori). The pulsewidth, wavelength, and repetition frequency of the dye laser are 0.3 ps, 642 nm, and 76 MHz, respectively. The output light (~200 mW) was attenuated by neutral density filters to a few milliwatts and focused by a lens ( $f=200$  cm) on the sample. The focused spot had a diameter of about 0.3 mm at the sample. The sample was mounted in a cryostat whose temperature could be changed from room temperature to about 10 K. The emitted fluorescence from the sample was first focused by a lens on the input slit of a spectrometer, which wavelength-resolved it. The output from the spectrometer was then time-resolved by a synchroscan streak camera (Hamamatsu Pho-

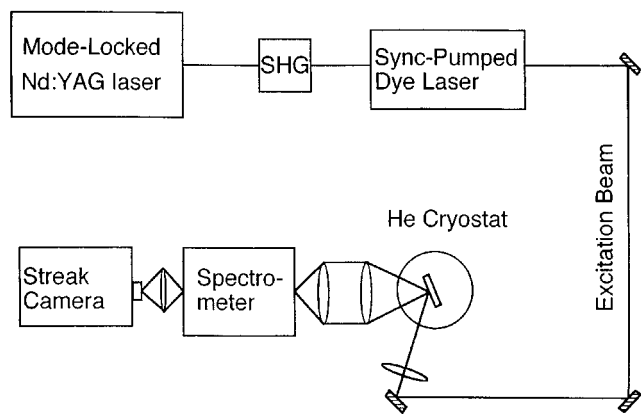


FIG. 2. Schematic diagram of the experiment.

tonics Model M1955). Therefore, from the output of the camera, we could get time-resolved spectrum of the fluorescence emitted by the sample. The resolution time of the streak camera is about 10 ps. No deconvolution of observed decay functions was performed since both the resolution time of the system and the excitation pulsewidth were much smaller than the decay time constants of fluorescence in our experimental situation.

#### A. MG doped in polymer glass

The absorption spectra of malachite green doped in PMMA polymer are shown in Fig. 3. The solid curve shows the spectrum at room temperature (290 K), and the dashed curve shows the spectrum at low temperature (11 K). The excitation wavelength (642 nm) is indicated by an arrow. The spectrum at low temperature is quite similar to the one at room temperature except for a narrowing of the spectrum due to a reduction of homogeneous width at low temperature.

The fluorescence decay curves of malachite green doped in PMMA as observed by the streak camera system are shown in Fig. 4. The observation wavelength is 670 nm. No

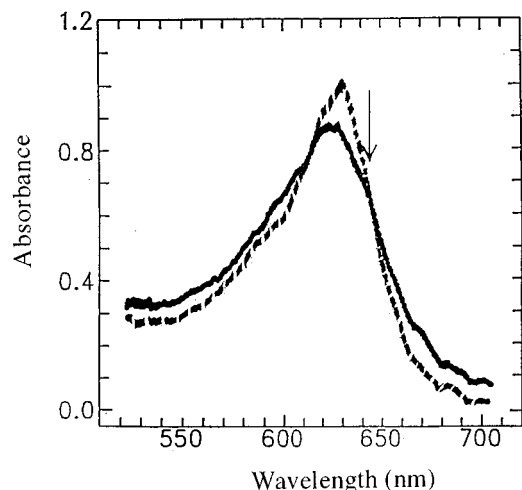


FIG. 3. Absorption spectra of MG/PMMA at room temperature 290 K (solid curve) and at low temperature 11 K (dashed curve). The arrow indicates the excitation wavelength of the laser (642 nm).

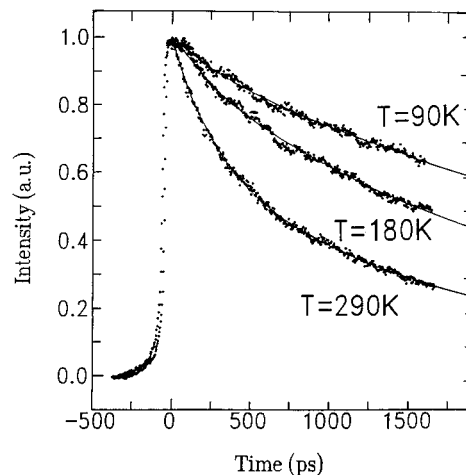


FIG. 4. Fluorescence decay curves of MG/PMMA as functions of temperature. The observation wavelength is 670 nm. Solid curves are least-squares fits by biexponential functions:  $I(t) = A_1 \exp(-t/\tau_1) + A_2 \exp(-t/\tau_2)$ , where  $\tau_1$  and  $\tau_2$  are the fast and slow time constants, and  $A_1$  and  $A_2$  are the respective amplitudes.

wavelength dependence of the decay curves was observed in our experiment. The curves are not single exponentials but can be well fitted by biexponential functions [ $I(t) = A_1 \exp(-t/\tau_1) + A_2 \exp(-t/\tau_2)$ ], with amplitudes  $A_1$  and  $A_2$  and time constants  $\tau_1$  and  $\tau_2$ . As the temperature is lowered, the decay becomes slower and the amplitude of the fast component  $A_1$  decreases.

Figure 5 shows the decay time constants  $\tau_1$  and  $\tau_2$  of the biexponential fit as functions of temperature. The fast decay time constant  $\tau_1$  (triangle) is seen to be almost independent of temperature and the slow decay time constant  $\tau_2$  (dot) is seen to increase slowly as the temperature is lowered. We did not plot the values of  $\tau_1$  at very low temperatures because the amplitude of the fast component becomes very small at low temperatures and reliable values of  $\tau_1$  become difficult to obtain.

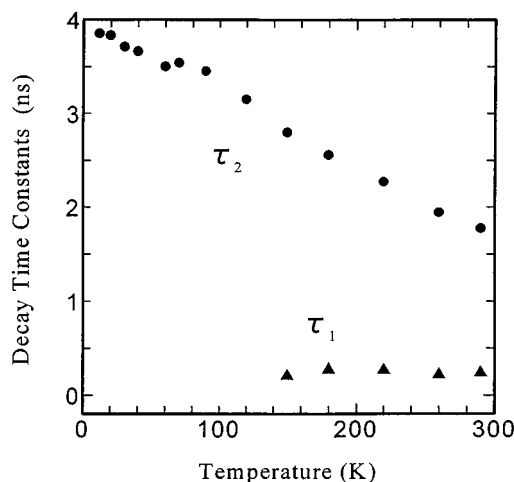


FIG. 5. Fast and slow decay time constants ( $\tau_1$  and  $\tau_2$ ) of the biexponential decay plotted as functions of temperature for MG/PMMA. From the extrapolated value of  $\tau_2$  at 0 K, we obtain a radiative lifetime of  $\tau_r = 3.8$  ns.

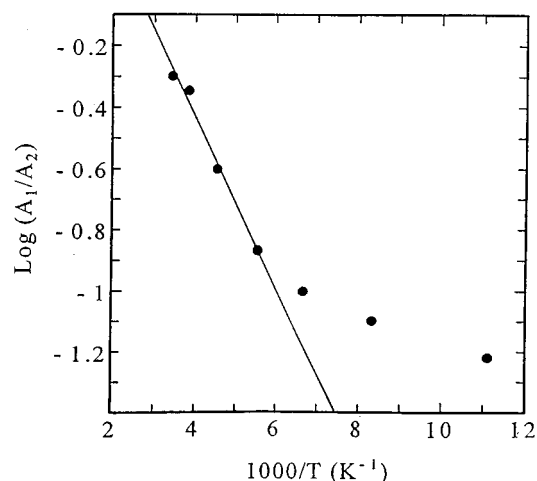


FIG. 6. Arrhenius plot of the amplitude ratio of the fast and slow components ( $A_1/A_2$ ) as a function of temperature for MG/PMMA. From the slope of the Arrhenius plot in the higher temperature range, we obtain a site energy difference of 1.2 kcal/mol.

The fluorescence decay time of MG is strongly dependent on the friction exerted by the surrounding molecules, and it is well known that polymer matrix is inhomogeneous and has a lot of voids in it. Therefore, the biexponential decay behavior of the fluorescence can be attributed to the site dependence of the doped molecule. We consider that the fast decay component arises from sites in the polymer where malachite green molecules are loosely bound to the surrounding matrix. At the loosely bound site, the phenyl rings can rotate rather freely in the matrix with relatively small activation energy. If the activation energy is smaller than  $k_B T$ , it is consistent with the very weak temperature dependence of  $\tau_1$ . On the other hand, the dominant slow decay component is considered to arise from sites where the molecules are tightly bound to the polymer matrix and is thought to represent the viscosity-dependent retardation of the phenyl ring rotations in the polymer. As the temperature is lowered, the rotational motions of the phenyl rings are progressively retarded, but even at quite low temperatures (e.g., near 100 K), appreciable motions of the phenyl rings can be observed. At extremely low temperatures, the decay is limited by the radiative lifetime  $\tau_r$  of the dye in PMMA. From the extrapolated value of  $\tau_2$  at 0 K, we estimate a radiative lifetime of  $\tau_r = 3.8$  ns for malachite green doped in PMMA.

The Arrhenius plot of the ratio of the amplitudes of the fast and slow components ( $A_1/A_2$ ) is shown in Fig. 6. As the temperature is increased, the amplitude of the fast component increases very much. If we assume thermal equilibrium, the free energy difference between the two types of sites estimated from the slope in the higher temperature range (where the ratio  $A_1/A_2$  changes significantly), is found to be about 1.2 kcal/mol.

The biexponential or multiexponential decay behavior of TPM dyes in liquids were experimentally observed by some authors<sup>6,8</sup> and theoretically predicted by BFO<sup>21</sup> and Ben-Amotz and Harris.<sup>17,18</sup> But the decay time in polymers is much longer than that in liquids, and the strong temperature dependence of  $A_1/A_2$  and the very weak temperature depen-

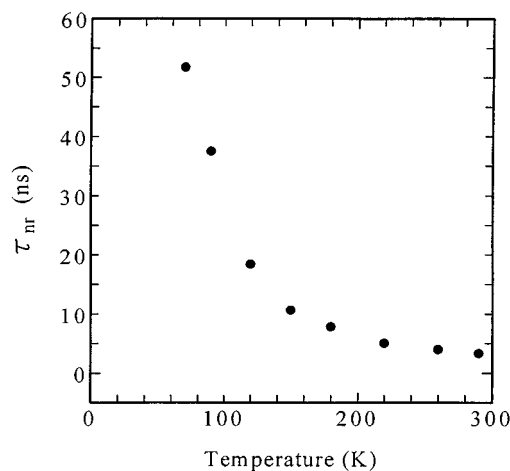


FIG. 7. Nonradiative lifetime ( $\tau_{nr}$ ) plotted as a function of temperature for MG/PMMA.

dence of fast decay time  $\tau_1$  are not consistent with their predictions. From the above reasons and the well known fact of the existence of inhomogeneity and voids in polymers, we consider that the fast and slow decay components originate from the loosely and tightly bound sites in polymers, respectively.

Since we consider that the slow sites represent the microviscosity of the polymer to phenyl ring rotations, we calculate nonradiative lifetime  $\tau_{nr}$  associated with the slow sites from  $\tau_2$ , by subtracting the effect of radiative lifetime,

$$\tau_{nr} = (\frac{1}{\tau_2} - \frac{1}{\tau_r})^{-1}, \quad (1)$$

where  $\tau_r = 3.8$  ns for malachite green in PMMA. The values of  $\tau_{nr}$  are plotted as a function of temperature in Fig. 7. As the temperature is decreased from room temperature to about 90 K, the nonradiative decay time increases by more than one order of magnitude.

As an example of different polymer, we doped MG in polyvinyl alcohol (PVA) and performed a similar type of experiment. As was the case in PMMA, the fluorescence decay curves were not single exponential but could be well fitted by biexponential functions. The fast and slow decay time constants ( $\tau_1$  and  $\tau_2$ ) of the biexponential fitting are shown as functions of temperature in Fig. 8. The values of fast time constant  $\tau_1$  were not plotted at low temperatures since the amplitude of the fast component became very small. As in PMMA, the fast time constant  $\tau_1$  is almost independent of temperature and the slow time constant  $\tau_2$  gradually decreases as the temperature is increased. The values of  $\tau_2$  are somewhat smaller than those of PMMA at the same temperature. From the extrapolated value of  $\tau_2$  at 0 K, we estimate a radiative lifetime of  $\tau_r = 2.3$  nsec for MG in PVA. The free energy difference between the fast and the slow site in PVA can be obtained from the Arrhenius plot of the amplitude ratio of the two components ( $A_1/A_2$ ), and we estimate an energy difference of 2.3 kcal/mol which is of the same order in the value obtained for MG in PMMA (1.2 kcal/mol).

The nonradiative decay time ( $\tau_{nr}$ ) associated with the dominant slow component  $\tau_2$  is calculated using Eq. (1). The

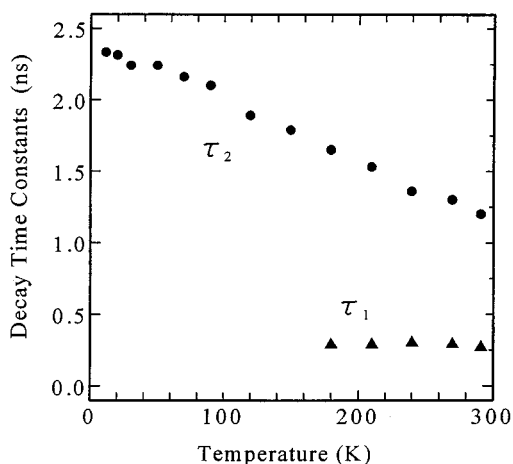


FIG. 8. Fast and slow decay time constants ( $\tau_1$  and  $\tau_2$ ) of the biexponential decay plotted as functions of temperature for MG/PVA. From the extrapolated value of  $\tau_2$  at 0 K, we obtain a radiative lifetime of  $\tau_r=2.3$  ns.

values of  $\tau_{nr}$  are plotted as a function of temperature in Fig. 9. As in PMMA, we observe a considerable increase of non-radiative lifetime as the temperature is lowered from room temperature to about 90 K.

The two examples (PMMA and PVA) concern the dynamics of phenyl rings of malachite green in polymers. As an example of a matrix very different from polymers we tried ethanol monomer glass.

### B. MG doped in monomer glass

The ethanol solution of malachite green was sealed in a glass cell with inner thickness of 1mm. The concentration of MG was about  $6 \times 10^{-5}$  M. To form the glass, the sample was first rapidly cooled down to 10 K and the measurements were performed while gradually raising the temperature. In the low temperature range up to about 110 K, the decay curves could be well fitted by single exponential functions with the slow decay time  $\tau_2$ . Above this temperature the amplitude of the fast component increased with temperature. At about 125 K, microcrystals began to form in the sample, and the crystals started to melt at about 150 K. The fast

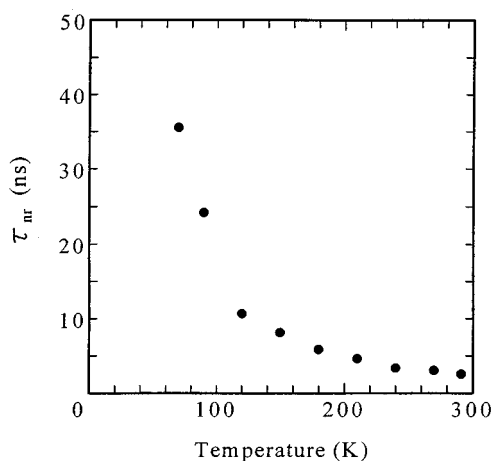


FIG. 9. Nonradiative lifetime ( $\tau_{nr}$ ) plotted as a function of temperature for MG/PVA.

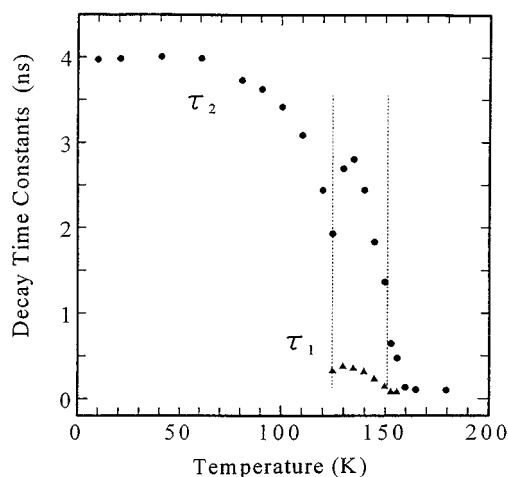


FIG. 10. Fast and slow decay time constants ( $\tau_1$  and  $\tau_2$ ) as functions of temperature for MG/ethanol. The region of opacity of the sample is indicated by two dashed lines. The melting point of ethanol is about 158 K.

component became dominant over the slow component above the melting temperature. The fast and slow decay time constants  $\tau_1$  (triangle) and  $\tau_2$  (dot) are plotted as functions of temperature in Fig. 10. The values of  $\tau_1$  above 155 K are not plotted because we could not get the reliable value in the present experiment.

The sample became opaque by the formation of microcrystals, and the temperature region of opacity is indicated by the two dashed lines. Biexponential nature of the decay curve was pronounced around the phase transition temperatures where coexistence of different phases is possible. In our recent measurements of fluorescence decay time of MG in noncrystallizing glass-forming monomers, the biexponential decay curves appeared near the glass transition temperatures. The study of glass transition by using MG optical microprobes will be discussed in our forthcoming paper.

The decay time  $\tau_2$  changes over a very wide range, but the change is dramatic in the neighborhood of the melting point which is about 158 K. From 10 to about 60 K, there is a plateau region of the curve where the decay time change is negligible. Here the phenyl rings of MG are thought to be strongly arrested because they are tightly packed among the small monomer units, in sharp contrast with the loose, long chained polymers. In polymers, we observe a sloping region for  $\tau_2$  even at quite low temperatures (see Figs. 5 and 8). From this plateau region, we obtain a radiative lifetime of  $\tau_r=4.0$  ns for MG/EtOH glass system. As the temperature is gradually increased above 70 K, the glass softens and the phenyl rings start to rotate. We therefore see a gradual drop of  $\tau_2$ . At about 125 K, microcrystals begin to form in the glass and the formation of microcrystals hinders the rotation of the phenyl rings, increases the microviscosity and we see a sudden increase of  $\tau_2$ . Above about 150 K, the crystals themselves start to melt, and the microviscosity suddenly drops to a very low value and so does  $\tau_2$ .

Using Eq. (1) values of  $\tau_{nr}$  are calculated from  $\tau_2$  and the radiative lifetime  $\tau_r (=4.0$  ns). The nonradiative decay rate  $\tau_{nr}^{-1}$  is shown as a function of temperature in Fig. 11. We observe that the decay rate changes by more than two orders

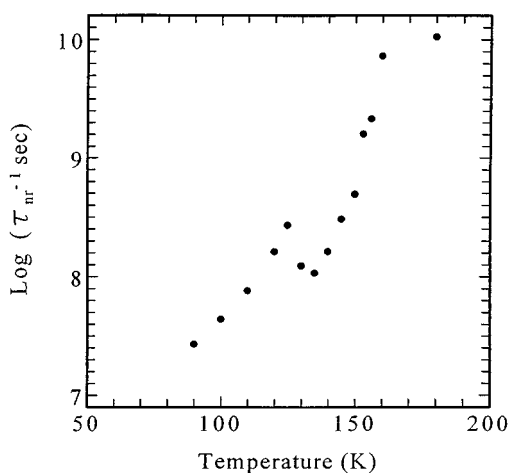


FIG. 11. Nonradiative decay rate ( $\tau_{nr}^{-1}$ ) as a function of temperature for MG/ethanol.

of magnitude as the temperature is changed by about 100 K around the melting point of ethanol.

### III. DISCUSSION

In this study, we have experimentally monitored the diffusive torsional motions of the phenyl rings of malachite green dye molecules in different solid matrices by measuring the fluorescence decay time as functions of temperature. From the temperature dependence of the slower time constant  $\tau_2$ , we have seen that in polymers, the phenyl rings can rotate quite rapidly even at very low temperatures. The rotational relaxation time (nonradiative decay time  $\tau_{nr}$ ) is of the order of  $10^{-8}$  s in PMMA and PVA at a temperature of about 100 K. The nonradiative decay time at room temperature is about one order of magnitude shorter.

There are many examples of photoisomerization experiments for stilbene, azobenzene, and spirobenzene molecules in polymers.<sup>31-34</sup> In all these cases, the relevant isomerization processes (e.g., *cis-trans* isomerization of azobenzene) involve large-scale sweeping motions of phenyl rings and other associated atoms and involve considerable displacements of the polymer material around these molecules. In the case of malachite green, the motion of the phenyl rings involves a rotational motion of only about 10 degrees around their axes and does not require a drastic motion of polymer material as is the case for the above-mentioned molecules. As a consequence of this fact and due to the barrierless nature of the phenyl ring rotation, the reaction (internal conversion) rate of malachite green in polymers can be much faster than the corresponding reaction rates of the above-mentioned molecules in polymers.

In the following we discuss the diffusive torsional dynamics of the phenyl rings by using the concept of microviscosity which has been used to describe the depolarization of chromophore molecules in polymers.<sup>27-29</sup> And the theoretical predictions are compared with the present experimental results.

### A. Theoretical considerations

It is now generally accepted that the excited-state potential surface of TPM dyes is barrierless.<sup>4</sup> There are a few theoretical treatments to describe the dynamics on a barrierless potential. For example, Bagchi, Fleming, and Oxtoby assumed a parabolic downhill potential surface,<sup>21</sup> while Ben-Amotz and Harris assumed a horizontal potential surface.<sup>17,18</sup> The difference between these two assumptions seems to be represented by whether the potential is downhill or horizontal toward a position where the excited state population is annihilated by internal conversion.

As long as decay curves can be well fitted by single exponentials, just as in our case for each of the slow or fast sites, the decay constant obtained should be nearly equal to the decay constant in the steady state realized when excited states are steadily supplied. The decay curves close to single exponential functions can actually be obtained from the theory by Ben-Amotz and Harris<sup>17,18</sup> for reasonable conditions as will be shown later. Theoretically, the decay constant in the steady state can relatively easily be obtained in comparison with that in the time-resolved situation as performed in the present experiment. The difference in the temperature dependence of the nonradiative decay rate between the two cases of downhill and horizontal potentials can clearly be presented by the steady-state theory as shown in the Appendix. From the steady-state theory we see that for downhill potential case the temperature dependence of the nonradiative decay rate can be expressed in a same form whether the potential is parabolically downhill as in the BFO model or linearly downhill.

In the case of diffusive rotations of phenyl rings in the excited state of malachite green molecules, internal conversion to the ground state takes place when phenyl rings rotate about 10 degrees from the angle just after excitation.<sup>4</sup> For rotations in the opposite direction, it is reasonable to consider that there exists an angle beyond which rotation is inhibited due to steric hindrance. This situation can be represented by a sink-diffusion problem where particles supplied from a source at a certain position meet a sink for their annihilation when they diffuse forward, but meet a wall for their reflection when they diffuse backward. The rate constant in the steady state in this problem was theoretically investigated in the Appendix. According to Eq. (A26) therein, the temperature dependence of the steady-state decay constant  $k_S$  is described by

$$k_S \propto D/T, \quad \text{in the downhill potential case,} \quad (2)$$

where  $D$  represents the diffusion constant and  $T$  the temperature. According to Eq. (A24), it is given by

$$k_S \propto D, \quad \text{in the horizontal potential case.} \quad (3)$$

The hydrodynamic Stokes-Einstein relation tells us that  $D$  is proportional to  $T/\eta$  where  $\eta$  represents the viscosity. For rotational diffusion, to be more exact, the relationship for the stick boundary condition is expressed as

$$D = k_B T / (24 \pi \eta R^3), \quad (4)$$

when the rotational motion is modeled as that of a sphere of hydrodynamic radius  $R$  around its axis. In the situation

where a decay constant is obtained as a good approximation, the decay time is given by the inverse of the decay constant, which behaves as in Eqs. (2) or (3). Taking into account Eq. (4) in these equations, we get the temperature dependence of the decay time  $\tau_{nr}$  as

$$\tau_{nr} \propto \eta, \quad \text{in the downhill potential case,} \quad (5)$$

or

$$\tau_{nr} \propto \eta/T, \quad \text{in the horizontal potential case.} \quad (6)$$

The long-time decay constant in the theory of Bagchi, Fleming, and Oxtoby<sup>21</sup> agrees with the temperature dependence shown in Eq. (5), since the potential assumed by them is downhill toward a sink. They assumed additionally that the potential rises quadratically from a sink as a function of the rotation angle. Even in this case, it can be regarded as an example of downhill potential cases as long as the initial position of supply is sufficiently apart from the sink, and the decay time obtained behaves in the same way as shown in Eq. (5). When the initial position of the supply is very close to the sink and the excess energy of the initial position compared to the sink is less than  $k_B T$ , the parabolic potential of the BFO model can be regarded as a nearly horizontal potential. In general the BFO model predicts a multi-exponential relaxation of the excited state population and in some conditions gives decay curves which are close to bi-exponential decay functions. But in these cases the fast decay constant changes with viscosity and temperature almost in the same way as the slow decay constant which is in marked contrast to our experimental result that although the slow decay time  $\tau_2$  changes with temperature, the fast decay time  $\tau_1$  is almost independent of temperature.

It will be shown later in the present work that for internal conversion of malachite green molecules in the excited state, the temperature dependence of the decay time can be more reasonably explained by Eq. (6), not by Eq. (5). This indicates that diffusive rotations of phenyl rings of these molecules take place on a horizontal potential surface. The potential relevant to this case is shown in Fig. 12(a) as a function of the coordinate  $x$  which represents the angle of rotation of phenyl rings from the angle where the malachite green molecule is excited. Then, a source for excited molecules is located at  $x=0$  on the potential. At an edge of the potential, a sink is present at  $x=d_s$  where internal conversion takes place. At the opposite edge, a wall for reflection is present at  $x=-d_w$  beyond which the rotation is inhibited due to steric hindrance. This problem is equivalent to the problem shown in Fig. 12(b) where diffusing particles can move beyond  $x=-d_w$  since no wall exists there, but they meet a sink at  $x=-2d_w-d_s$ , which exists additionally to the original sink at  $x=d_s$ . The diffusion in the newly added region of  $x$  for  $-2d_w-d_s < x < -d_w$  replicates that after reflection at the wall in the original problem of Fig. 12(a).

The survival probability of excited malachite green molecules still remaining after a pulse excitation at time zero is written as  $P(t)$  as a function of time  $t$  ( $\geq 0$ ) with  $P(0)=1$ . In the problem of Fig. 12(b),  $P(t)$  can be obtained by integrat-

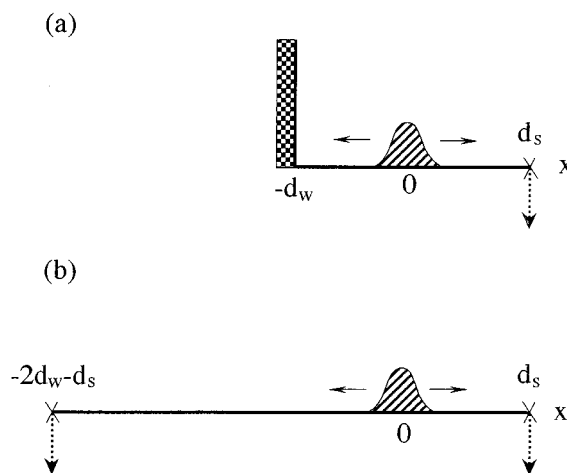


FIG. 12. (a) A horizontal potential surface with a wall at  $x=-d_w$ . The hatched region indicates a diffusing packet of excited-state population. The dotted arrow indicates the position of sink to the ground state. (b) Equivalent horizontal potential model where the wall is replaced by an image of the sink at  $x=-d_s-2d_w$ .

ing the distribution function over the entire region of  $x$  for  $-2d_w-d_s < x < d_s$ . This process was performed by Ben-Amotz and Harris<sup>17</sup> to give

$$P(t) = \frac{4}{\pi} \left[ \cos(\theta_0) \exp(-t/\tau_0) - \frac{1}{3} \cos(3\theta_0) \exp(-3^2 t/\tau_0) + \frac{1}{5} \cos(5\theta_0) \exp(-5^2 t/\tau_0) - \dots \right], \quad (7)$$

with

$$\theta_0 = \frac{\pi}{2} \frac{d_w}{d_w + d_s} \left( < \frac{\pi}{2} \right), \quad \tau_0 = \frac{4}{\pi^2} \frac{(d_w + d_s)^2}{D}, \quad (8)$$

where  $D$  represents the diffusion constant for rotational diffusion appearing also in Eqs. (2)–(4). The equivalence between Eq. (10) in Ref. 17 and Eq. (7) shown above can easily be checked by the replacement of  $x_0$  and “ $a$ ” in Ref. 17 by  $d_s$  and  $2(d_w + d_s)$ , respectively.

As mentioned before,  $d_s$  corresponds to an angle of about 10 degrees. Although  $d_w$  is unknown, it is reasonable to consider that  $d_w$  has a magnitude of the same order as  $d_s$ . In this case,  $|\cos 3\theta_0|$  in Eq. (7) has a magnitude of the same order as  $\cos \theta_0$ . Then, except for the very early time region, the second and the higher terms in the square bracket on the right-hand side of Eq. (7) can be neglected in comparison with the first term, since they decay much faster than the first term, with decay constants at least nine times as large as that for the first term. Moreover, if the sign of the second term of Eq. (7) is opposite to that of the first term, the second term mostly contributes only to the rounding off of the decay curve in the very early time region. In this situation,  $P(t)$  of Eq. (7) can adequately be regarded as showing a single-exponential decay where the decay time can be approximated by  $\tau_0$  in Eq. (8). It is a matter of course that  $\tau_0$  with  $D$

herein given by Eq. (4) reproduces Eq. (6). Thus the nearly single-exponential decay can be supported also theoretically on the basis of Eq. (7).

When the distance between the source and the wall is much larger than that between the source and the sink, that is, when  $d_w \gg d_s$ , then  $P(t)$  (survival probability) of Eq. (7) deviates significantly from a single exponential decay function, since  $\cos \theta_0$  is much smaller than unity. This case corresponds to the very asymmetrical placement of the two sinks about the source in the theory of Ben-Amotz and Harris.<sup>17</sup> They pointed out that in this case the decay becomes nearly biexponential with two time constants, both proportional to  $(\eta/T)$ . It is seen from Eq. (7) that  $P(t)$  changes with temperature only through the rescaling of time  $t$  by  $\tau_0$ . Since we observed strong changes in the form of the excited-state decay curves in each polymer by changing the temperature (the ratio  $A_1/A_2$  is strongly temperature-dependent and the temperature dependencies of  $\tau_1$  and  $\tau_2$  are very different), then it follows that, within the framework of Ben-Amotz and Harris' theory, the biexponential nature of the decay is not a consequence of the very asymmetrical placement of the sinks. Therefore, we assume that the sinks are not very asymmetrical about the initial excited-state population and the biexponential nature of the decay in our experiment was considered to arise from site dependence of malachite green molecules in the heterogeneous polymer matrix.

Oster and Nishijima<sup>3</sup> estimated the decay time for internal conversion by a time  $\tau_{ON}$  when the average spread of the rotation angle of phenyl rings reaches a certain value, in the present notation,  $d_s$  in the course of diffusion on a horizontal potential surface. When  $D$  represents the diffusion constant for rotational diffusion, as before, this means

$$\tau_{ON} = \frac{1}{2} d_s^2 / D. \quad (9)$$

It is reasonable that  $\tau_{ON}$  has a magnitude of the same order as  $\tau_0$  in Eq. (8) and has the same temperature dependence as shown in Eq. (6) when  $D$  of Eq. (4) is used in Eq. (9).

It seems instructive to point out the origin of the difference between the cases in Eqs. (2) and (3). In the case of Eq. (3), it is apparent from Eq. (9) that  $k_S$  represents the speed of diffusional spread of the distribution initially localized at a certain point on a horizontal potential surface. In the case of Eq. (2), on the other hand,  $k_S$  represents the speed of drift motion of the whole distribution in the force field of a downhill potential.

### B. Microviscosity of polymer

In order to obtain the microviscosity of the polymer matrices to the phenyl ring rotation from experimental data, we first use the result for downhill potential, which shows that the nonradiative decay time is simply proportional to the microviscosity [Eq. (5)]. If we assume such a relationship, then we can calculate the relative microviscosity of the polymer as a function of temperature from the relation

$$\eta / \eta_{ref} = \tau / \tau_{ref}, \quad (10)$$

where the subscript "ref" indicates the values at an arbitrary reference temperature  $T_{ref}$ . Here, the symbol  $\tau$  indicates only

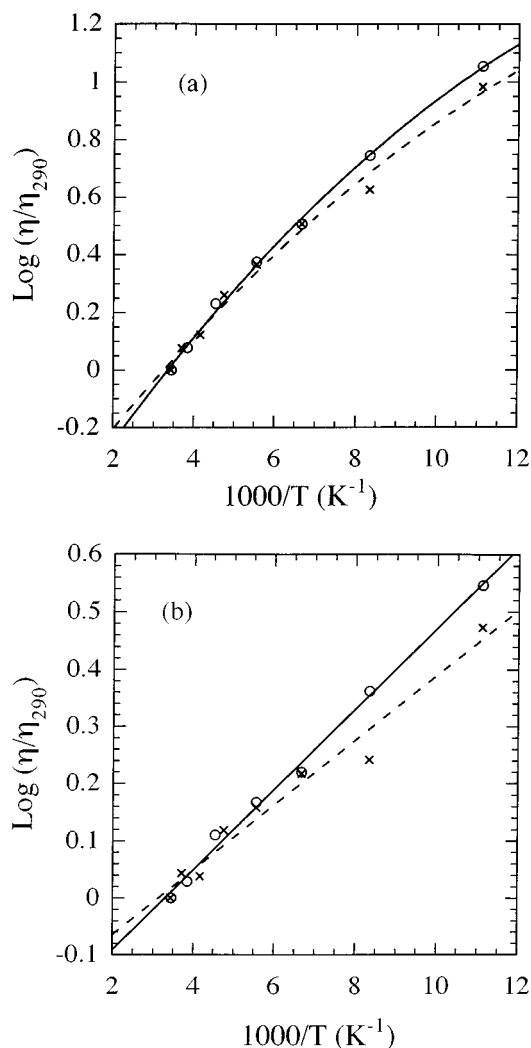


FIG. 13. Arrhenius plots of relative microviscosity if the excited-state potential surface is assumed to be downhill (a), and if the excited-state potential is assumed to be horizontal (b) for MG/PMMA (open circle) and for MG/PVA (cross).

the nonradiative part of the decay time as calculated from Eq. (1). For MG doped in PMMA and PVA, we take them as  $T_{ref} = 290$  K. If we assume such a relation, and calculate the microviscosity of PMMA (open circle) and PVA (cross) to the phenyl ring rotation, then the Arrhenius plots of microviscosity will look like Fig. 13(a). These Arrhenius plots are clearly curved and are not straight lines. It means that the microviscosity does not have a definite activation energy.

On the other hand, if we assume that the potential surface is horizontal, then the nonradiative decay time is proportional to  $\eta/T$  [Eq. (6)], and the relative microviscosity can be calculated from the relation,

$$\eta / \eta_{ref} = (\tau / \tau_{ref})(T / T_{ref}). \quad (11)$$

The Arrhenius plots of microviscosity calculated from the above equation are shown in Fig. 13(b) for MG in PMMA (open circle) and PVA (cross). In contrast to Fig. 13(a), both of these plots are very nearly straight lines. This means that the microviscosity of the polymer to the phenyl ring rotations has a fixed activation energy and obeys the Andrade equation

TABLE I. Energies determined in the experiment.

Matrix	Activation energy of microviscosity (kcal/mol)	Site energy difference (kcal/mol)
PMMA	0.33	1.2
PVA	0.26	2.3

$$\eta = \eta_0 \exp\left(\frac{E_a}{k_B T}\right). \quad (12)$$

This equation is obeyed by many liquids over a wide range of temperature, as first shown by Andrade.<sup>35,36</sup> It is known that in long chained polymers, the microviscosity experienced by a small doped molecule is very much different from the bulk macroviscosity.<sup>26–29</sup> But the above result means that, the microscopic viscosity itself obeys an equation very similar to the one obeyed by the macroscopic viscosity of many liquids. The activation energies of microviscosity  $E_a$  can be estimated from the slope of Arrhenius plots and are found to be about 0.33 kcal/mol for MG/PMMA and 0.26 kcal/mol for MG/PVA. If we assume any other potential surface which is significantly different from a horizontal one, the Arrhenius plot of microviscosity will not be a straight line. A horizontal potential surface seems to be the most reasonable one, since it would give an Arrhenius type dependence of microviscosity obeyed by many liquids. A horizontal potential for the excited state of a TPM dye, crystal violet, was also shown by Ben-Amotz and Harris<sup>17</sup> to result in a better fit to experimental data than a parabolic potential for certain liquids.

In the above, for both PVA and PMMA, we assumed that the potential surface is horizontal and the motion of the phenyl rings on the  $S_1$  excited-state of malachite green in polymer solids is controlled by diffusion, and calculated microviscosity from the experimentally determined fluorescence lifetime. Then the Arrhenius plot of the microviscosity was found to be a straight line and the temperature dependence of the microviscosity obeys an equation which is also obeyed by many liquids. The implication of this result is that as far as the local microscopic dynamics of a solid polymer is concerned, it behaves in a way similar to many liquids.

The activation energies of microviscosity determined from Arrhenius plots are shown in Table I. The table also shows the free energy differences between the fast and slow sites for the two polymers.

### C. Microviscosity of monomer

Assuming a horizontal excited-state potential surface, and setting  $T_{\text{ref}} = 156$  K, the relative microviscosity was calculated from  $\tau_{\text{nr}}$  for the case of MG doped in ethanol glass. The Arrhenius plot of microviscosity is shown in Fig. 14. The overall plot is not a straight line. From this, we conclude that the microviscosity of ethanol in its phase transition region does not have a fixed activation energy. This is reasonable, since the change of microviscosity is caused by phase transition of ethanol and the activation energy of viscosity itself is not constant during this process. But in this case, we can monitor the change of microenvironment as the glass

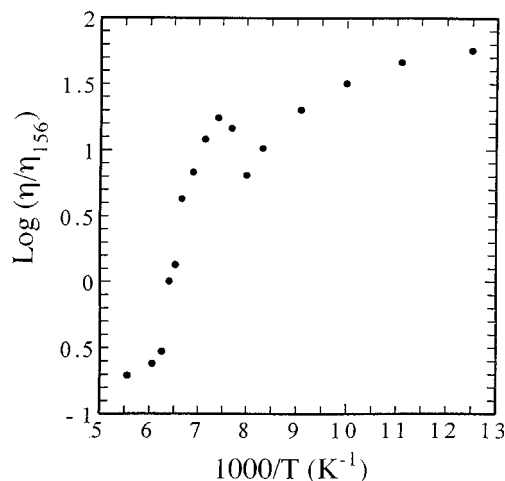


FIG. 14. Arrhenius plot of relative microviscosity for MG/ethanol.

passes through its phase transition. The change in microenvironment is reflected in the microviscosity of the medium with respect to the rotational motion of the phenyl rings. The effects of glass softening, microcrystallization and melting were all reflected in the fluorescence decay time of malachite green molecules.

The microviscosity is seen to vary by several hundred times as the temperature is varied by about 100 K around the melting point of ethanol. This is to be contrasted with a microviscosity change of several times in polymers (PMMA or PVA) over a temperature range of about 200 K. The difference is due to the drastic nature of the structural change in ethanol from solid to liquid during its phase transition as compared to a very gradual change in solid polymers which are already well below their glass transition temperatures.

It is a remarkable fact that the excited-state lifetime of malachite green changes by about three orders of magnitude, from a few picoseconds<sup>4,13</sup> in low-viscosity solvents to a few nanoseconds in polymers. This fact shows that the rotation of the phenyl rings, which causes the internal conversion process, is very much dependent on the immediate surroundings of the molecules. Moreover, the internal potential barrier of these molecules are already shown to be zero or extremely small, and the potential surface is considered to be horizontal, and so the molecules can serve as good probes of their immediate surroundings. Hence we propose that malachite green molecules can be used as sensitive optical (fluorescent) microprobes to investigate the phase transition processes of glasses and other substances.

### IV. CONCLUSION

In this paper, we have studied the torsional dynamics of a triphenylmethane (TPM) dye, malachite green, in polymeric and monomeric glasses. We believe that to the best of our knowledge, this is the first detailed study of time-resolved excited-state dynamics of TPM dyes in solid systems. We observed that the phenyl rings of malachite green rotate diffusively in the polymer matrix quite rapidly even at low temperatures but cannot rotate rapidly in monomer glass once freezing is complete. We compared the results of the

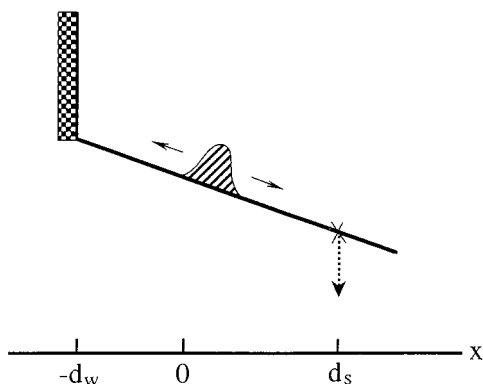


FIG. 15. A downhill potential surface with a wall at  $x = -d_w$ . A sink is located at  $x = d_s$ .

reaction-rate theory with our experimental results, and suggest that the excited-state potential surface of malachite green is horizontal or nearly so, and the rotation of the phenyl rings on this surface can be described by a diffusive motion characterized by a microviscosity of the host. The microviscosity of polymers to the phenyl ring rotation has a definite activation energy and obeys the Andrade equation, which is also obeyed by many liquids. We also propose, using the example of ethanol glass, that malachite green or similar TPM dyes can be used as sensitive optical microprobes to monitor the phase transition of glasses or other similar systems if malachite green molecules can be dispersed into them.

### APPENDIX: STEADY-STATE REACTION RATE THEORY

Let us consider here a sink-diffusion problem in which particles diffuse on a potential, in general, with a nonvanishing slope, before being annihilated at a sink. The situation is described in Fig. 15. The potential is represented by  $V(x)$ , which is a function of the coordinate  $x$  for diffusing particles which are supplied from a source located at  $x=0$ . At the edges of this potential, there exist a sink of particles at  $x=d_s (>0)$  and a wall at  $x=-d_w (<0)$  where particles are reflected. The number of particles found in an infinitesimal interval from  $x$  to  $x+dx$  at time  $t$  is written as  $P(x,t)dx$ . Then,  $P(x,t)$  represents the distribution function. It satisfies the Smoluchowski equation describing diffusion in a potential field, in the present case,  $V(x)$  for  $-d_w < x < d_s$  as

$$\frac{\partial}{\partial t} P(x,t) = D \frac{\partial}{\partial x} \left[ \frac{\partial}{\partial x} + \frac{1}{k_B T} \frac{dV(x)}{dx} \right] P(x,t), \quad (A1)$$

where  $D$  represents the diffusion constant and  $T$  the temperature. Introducing

$$J(x,t) = -D \left[ \frac{\partial}{\partial x} + \frac{1}{k_B T} \frac{dV(x)}{dx} \right] P(x,t), \quad (A2)$$

we can cast Eq. (A1) into a form of the equation of continuity as

$$\frac{\partial}{\partial t} P(x,t) + \frac{\partial}{\partial x} J(x,t) = 0. \quad (A3)$$

Therefore,  $J(x,t)$  represents the current of particles at coordinate  $x$  at time  $t$ . When a particle arriving at the sink is surely annihilated, the boundary condition for the sink is

$$P(x,t) = 0, \quad \text{at } x = d_s. \quad (A4)$$

The boundary condition for the wall describes that the current vanishes there, as

$$J(x,t) = 0, \quad \text{at } x = -d_w. \quad (A5)$$

(a) When particles are supplied only at  $t=0$ , the initial condition for Eq. (A1) is

$$P(x,t) = \delta(x), \quad \text{at } t = 0. \quad (A6)$$

In this case, the survival probability of particles at time  $t$  is given by

$$P(t) = \int_{-d_w}^{d_s} P(x,t) dx, \quad \text{with } P(0) = 1, \quad (A7)$$

and it decays from unity as  $t$  increases from zero. Even in this case, if the time decay of  $P(t)$  can be approximated by a single exponential, the decay constant obtained should coincide with that obtained in the situation of steady state which is treated below. A concrete example of this relation is shown later.

(b) The steady state is realized under a condition of steady supply of particles from the source. In this state, the distribution function becomes independent of time  $t$  as

$$P(x,t) = P_S(x), \quad (A8)$$

where  $P_S(x)$  represents the steady-state distribution function. In the steady state, we have a steady current of particles from the source to the sink, and we get from Eq. (A2)

$$-D \left[ \frac{d}{dx} + \frac{1}{k_B T} \frac{dV(x)}{dx} \right] P_S(x) = J_S, \quad \text{for } 0 < x \leq d_s, \quad (A9)$$

where  $J_S$  represents the steady current independent of  $x$ . In the region from the source to the wall, on the other hand, we should have no current of particles, which is consistent with the boundary condition for the wall in Eq. (A5). Then, we get

$$-D \left[ \frac{d}{dx} + \frac{1}{k_B T} \frac{dV(x)}{dx} \right] P_S(x) = 0, \quad \text{for } -d_w \leq x < 0. \quad (A10)$$

The solution to Eq. (A10) is the thermal-equilibrium distribution in the potential  $V(x)$ . Then  $P_S(x)$  can be expressed as

$$P_S(x) = P_S(0) \exp \left[ -\frac{V(x) - V(0)}{k_B T} \right], \quad \text{for } -d_w \leq x \leq 0, \quad (A11)$$

where the steady distribution at the source  $P_S(0)$  was introduced as a constant of integration in solving Eq. (A10). The boundary condition for the sink in Eq. (A4) imposes

$$P_S(x) = 0, \quad \text{at } x = d_s. \quad (A12)$$

Since a nonvanishing current of particles exists in the region of  $0 \leq x \leq d_s$ , the steady-state distribution function in this region deviates from the thermal-equilibrium distribution function which is written as

$$P_e(x) = P_S(0) \exp\left[-\frac{V(x) - V(0)}{k_B T}\right], \quad \text{for } 0 \leq x \leq d_s, \quad (\text{A13})$$

in the same form as the right-hand side of Eq. (A11). Let us rewrite Eq. (A9) into

$$\frac{d}{dx} [P_e(x)^{-1} P_S(x)] = -\frac{J_S}{D} P_e(x)^{-1}, \quad (\text{A14})$$

by using  $P_e(x)$  of Eq. (A13). Integrating both sides of Eq. (A14) in  $x$  from 0 to  $x$ , we get

$$P_S(x) = P_e(x) - \frac{J_S}{D} P_e(x) \int_0^x P_e(y)^{-1} dy, \quad \text{for } 0 \leq x \leq d_s. \quad (\text{A15})$$

To proceed further ahead, we must indicate a concrete form of the potential  $V(x)$  which is required in the integration in  $y$  on the right-hand side of Eq. (A15) since  $P_e(x)$  is determined by  $V(x)$  in Eq. (A13). Let us take it so as to be the most simplified form of a downhill potential, which is linear in  $x$  as

$$V(x) = V(0) - cx, \quad \text{with } c \geq 0. \quad (\text{A16})$$

Then, Eq. (A16) enables us to perform the integration in Eq. (A15), to get

$$P_S(x) = \left[ P_S(0) - \frac{k_B T J_S}{c D} \right] \exp\left(\frac{cx}{k_B T}\right) + \frac{k_B T J_S}{c D}. \quad (\text{A17})$$

The still-unknown constant  $P_S(0)$  in Eq. (A17) can be determined by the boundary condition in Eq. (A12), as

$$P_S(0) = \frac{k_B T J_S}{c D} \left[ 1 - \exp\left(-\frac{c d_s}{k_B T}\right) \right]. \quad (\text{A18})$$

Introducing Eq. (A18) back to Eq. (A17), we get the steady-state distribution function as

$$P_S(x) = \frac{k_B T J_S}{c D} \left[ 1 - \exp\left(-\frac{c(d_s - x)}{k_B T}\right) \right], \quad \text{for } 0 \leq x \leq d_s. \quad (\text{A19})$$

Integrating the right-hand side of Eq. (A19) in  $x$  from 0 to  $d_s$ , we get the steady population of particles in the  $x$  region of  $0 \leq x \leq d_s$ . When it is written as  $P_+$ , it is given by

$$P_+ = \frac{J_S}{D} \left(\frac{k_B T}{c}\right)^2 \left[ \frac{c d_s}{k_B T} - 1 + \exp\left(-\frac{c d_s}{k_B T}\right) \right]. \quad (\text{A20})$$

The steady population in the  $x$  region of  $-d_w \leq x \leq 0$  can be obtained by integrating the right-hand side of Eq. (A11) where  $V(x)$  is given by Eq. (A16) and  $P_S(0)$  by Eq. (A18). When it is written as  $P_-$ , it is given by

$$P_- = \frac{J_S}{D} \left(\frac{k_B T}{c}\right)^2 \left[ 1 - \exp\left(-\frac{c d_w}{k_B T}\right) \right] \left[ 1 - \exp\left(-\frac{c d_s}{k_B T}\right) \right]. \quad (\text{A21})$$

The total steady-state population of particles is given by  $P_+ + P_-$ , while the number of particles annihilated per unit time at the sink is given by  $J_S$  as defined by Eq. (A9). Then, the steady-state decay constant is determined by  $J_S / (P_+ + P_-)$ . Written as  $k_S$ , it can be obtained from Eqs. (A20) and (A21) as

$$k_S = D \left(\frac{c}{k_B T}\right)^2 \left/ \left[ \frac{c d_s}{k_B T} - \exp\left(-\frac{c d_w}{k_B T}\right) + \exp\left(-\frac{c(d_w + d_s)}{k_B T}\right) \right] \right. \quad (\text{A22})$$

This formula for the steady-state decay constant is applicable for any value of the slope index  $c$  of the potential  $V(x)$  in Eq. (A16). Especially, the case of a nearly horizontal potential is defined by

$$1 - \exp\left[-\frac{V(-d_w) - V(d_s)}{k_B T}\right] \ll 1, \quad (\text{A23})$$

that is, by

$$c(d_w + d_s) / (k_B T) \ll 1. \quad (\text{A23}')$$

Under this condition,  $c d_w / (k_B T) \ll 1$  is automatically satisfied. Then, the steady-state decay constant of Eq. (A22) reduces to

$$k_S = \frac{2D}{d_s(d_s + 2d_w)}, \quad \text{in the horizontal-potential case.} \quad (\text{A24})$$

On the other hand, the case of a downhill potential is defined by

$$\exp\left[-\frac{V(-d_w) - V(0)}{k_B T}\right] \ll \frac{V(0) - V(d_s)}{k_B T}, \quad (\text{A25})$$

that is, by

$$\exp[-c d_w / (k_B T)] \ll c d_s / (k_B T). \quad (\text{A25}')$$

Under this condition,  $\exp[-c(d_w + d_s) / (k_B T)] \ll c d_s / (k_B T)$  is automatically satisfied. Then the steady-state decay constant of Eq. (A22) reduces to

$$k_S = \frac{c}{k_B T} \frac{D}{d_s}, \quad \text{in the downhill-potential case.} \quad (\text{A26})$$

Since the left-hand side of the inequality (A25) is always smaller than unity, it is surely satisfied when  $V(0) - V(d_s) \gg k_B T$ , that is, when the potential at the source is much higher than that at the sink in comparison with the thermal energy  $k_B T$ .

In the horizontal potential case, Ben-Amotz and Harris<sup>17</sup> have clarified the explicit expression for the time decay of the survival probability  $P(t)$  which is defined by Eq. (A7) when particles are supplied only at  $t=0$  under the initial condition in Eq. (A6). It was given by Eqs. (7) and (8) in the text. Then, it is instructive to show explicitly the relation between the steady-state decay constant given by Eq. (A24) and the average decay constant derived from  $P(t)$ , that is, the relation pointed out in the sentence following Eq. (A7). When the decay of  $P(t)$  can be approximated by a single exponential, the average decay constant can be derived by

$$k_A = 1 \left/ \int_0^\infty P(t) dt \right., \quad \text{with } P(0) = 1. \quad (\text{A27})$$

For  $P(t)$  given by Eq. (7) in the text, the integration in the denominator on the right-hand side of Eq. (A27) can analytically be performed by using a Fourier-series formula

$$\begin{aligned} & \cos\left(\frac{1}{2} \pi z\right) - \frac{1}{3^3} \cos\left(\frac{3}{2} \pi z\right) + \frac{1}{5^3} \cos\left(\frac{5}{2} \pi z\right) - \dots \\ & = \frac{\pi^3}{32} (1-z^2), \quad \text{for } |z| < 1. \end{aligned} \quad (\text{A28})$$

Then we can easily see that  $k_A$  given by Eq. (A27) coincides with  $k_S$  given by Eq. (A24).

The denominator on the right-hand side of Eq. (A27) has been called the first passage time, and represents the average lifetime of a particle before annihilation at the sink. Therefore,  $k_A$  of Eq. (A27) can be regarded as the average decay constant even if the decay of  $P(t)$  deviates significantly from single exponential, and it coincides with  $k_S$  of Eq. (A24) which can be calculated without explicit knowledge of the time decay of  $P(t)$ .

<sup>1</sup>J. Stark and P. Lipp, *Z. Phys. Chem.* **86**, 36 (1913).

<sup>2</sup>G. C. Schmidt, *Ann. Phys.* **65**, 247 (1921).

<sup>3</sup>G. Oster and Y. Nishijima, *J. Am. Chem. Soc.* **78**, 1581 (1956).

<sup>4</sup>D. Ben-Amotz and C. B. Harris, *J. Chem. Phys.* **86**, 4856, (1987).

<sup>5</sup>D. Madge and M. W. Windsor, *Chem. Phys. Lett.* **24**, 144 (1974).

<sup>6</sup>E. P. Ippen, C. V. Shank, and A. Bergman, *Chem. Phys. Lett.* **24**, 144 (1976).

<sup>7</sup>Y. Wu, F. Pellegrino, M. Grant, and R. R. Alfano, *J. Chem. Phys.* **67**, 1766 (1977).

<sup>8</sup>M. D. Hirsch and H. Mahr, *Chem. Phys. Lett.* **60**, 299 (1979).

<sup>9</sup>D. A. Cremers and M. W. Windsor, *Chem. Phys. Lett.* **71**, 27 (1980).

<sup>10</sup>D. Ben-Amotz and C. B. Harris, *Chem. Phys. Lett.* **119**, 305 (1985).

<sup>11</sup>T. Doust, *Chem. Phys. Lett.* **96**, 522 (1983).

<sup>12</sup>V. Sundstrom, T. Gillbro, and H. Bergstrom, *Chem. Phys.* **73**, 439 (1982).

<sup>13</sup>V. Sundstrom and T. Gillbro, *J. Chem. Phys.* **81**, 3463 (1984).

<sup>14</sup>D. J. Erskine, A. J. Taylor, and C. L. Tang, *J. Chem. Phys.* **80**, 5338 (1984).

<sup>15</sup>R. Menzel, C. W. Hoganson, and M. W. Windsor, *Chem. Phys. Lett.* **120**, 29 (1985).

<sup>16</sup>D. Ben-Amotz and C. B. Harris, in *Ultrafast Phenomena V*, edited by G. R. Fleming and A. E. Siegman (Springer, New York, 1986).

<sup>17</sup>D. Ben-Amotz and C. B. Harris, *J. Chem. Phys.* **86**, 5433 (1987).

<sup>18</sup>D. Ben-Amotz, R. Jeanloz, and C. B. Harris, *J. Chem. Phys.* **86**, 6119 (1987).

<sup>19</sup>T. Robl and A. Seilmeier, *Chem. Phys. Lett.* **147**, 55 (1988).

<sup>20</sup>M. M. Martin, E. Breheret, F. Nesa, and Y. H. Meyer, *Chem. Phys.* **130**, 279 (1989).

<sup>21</sup>B. Bagchi, G. R. Fleming, and D. W. Oxtoby, *J. Chem. Phys.* **78**, 7375 (1983).

<sup>22</sup>A. L. Huston, B. L. Justus, and A. J. Campillo, *Chem. Phys. Lett.* **122**, 617 (1985).

<sup>23</sup>M. Canva, G. Le Saux, P. Georges, A. Brun, F. Chaput, and J. P. Boilot, *Chem. Phys. Lett.* **176**, 495 (1991).

<sup>24</sup>M. Canva, G. Le Saux, P. Georges, A. Brun, F. Chaput, and J. P. Boilot, in *Chemical Processing of Advanced Materials* (Wiley, New York, 1992), Chap. 86.

<sup>25</sup>K. Kemnitz and K. Yoshihara, *J. Phys. Chem.* **94**, 8805 (1990).

<sup>26</sup>Y. Nishijima and Y. Saito, *Rept. Progr. Poly. Phys. Jpn.* **15**, 433 (1972).

<sup>27</sup>R. D. M. Neilson, I. Soutar, and W. Steedman, *Macromolecules* **10**, 1193 (1977).

<sup>28</sup>D. Barkowski, W. Mersch and Th. Dorfmueller, *J. Poly. Sci.: Poly. Phys. Ed.* **20**, 953 (1982).

<sup>29</sup>H. L. Ding, Ph.D. thesis, University of Southern California (1984).

<sup>30</sup>R. J. Goldacre and J. N. Philips, *J. Chem. Soc.* **2**, 1724 (1949).

<sup>31</sup>C. S. P. Sung, L. Lamarre, and M. K. Tse, *Macromolecules* **12**, 666 (1979).

<sup>32</sup>K. Horie, M. Tsukamoto, and I. Mita, *Eur. Polym. J.* **21**, 805 (1985).

<sup>33</sup>K. Horie, K. Hirao, N. Kenmochi, and I. Mita, *Makromol. Chem. Rapid Commun.* **9**, 267 (1988).

<sup>34</sup>T. Naito, K. Horie, and I. Mita, *Macromolecules* **24**, 2907 (1991).

<sup>35</sup>E. N. da C. Andrade, *Nature (London)* **125**, 309 (1930).

<sup>36</sup>E. N. da C. Andrade, *Philos. Mag.* **17**, 698 (1934).